Determining Flow Resistance through Vegetation Canopy

Ryan Falkenstein-Smith and Kevin McGrattan

National Institute of Standards and Technology
Gaithersburg, Maryland, USA

Corresponding Author: Ryan Falkenstein-Smith, ryan.falkenstein-smith@nist.gov

Abstract

This study documents the measurement of the wind resistance of different types of vegetation. The measurements are made in a wind tunnel with a 2.0 m test section and 0.5 m by 0.5 m cross- section. Samples of vegetation have been cut into cubical volumes that span the cross-section of the tunnel. The wind resistance is inferred via measurement of the pressure drop across the sample at wind speeds ranging from 2 m/s to 8 m/s. The average drag coefficient of all sample configurations was determined to be 2.8 with an expanded uncertainty of 0.4. A random-effects one-way ANOVA was implemented on the drag coefficients of different vegetation samples. The analysis yielded a significant variation among the species. Further examination using a Tukey's test, showed only a single difference between vegetation two species. Despite the significant difference, the average drag coefficient of each species was still within the uncertainty bounds of the overall average drag coefficient, suggesting that the significant difference may not be large enough to have a practical implication.

1 Introduction

The Fire Research Division of the National Institute of Standards and Technology (NIST) has developed several numerical models to predict the behavior of fires within buildings. One of the models, a computational fluid dynamics (CFD) code called the Fire Dynamics Simulator (FDS)[1], has been extended to model fires in the wildland-urban interface (WUI). One crucial component of this type of modeling is the proper treatment of wind-driven flow through vegetation. The objective of the experiments described in this work is to measure the drag coefficient of vegetation for an empirical sub-model appropriate for CFD.

Measurements of this type have been performed by other researchers[2–6], most of whom used wind tunnels of various sizes. In most cases, a single plant or small tree was positioned within the tunnel and the resistance force measured. However, such a measurement is not readily applicable to a CFD model which does not necessarily consider the tree as a whole but rather as a volume occupied by subgrid-scale objects that decrease the momentum of the gases flowing through. Some plants might be smaller than a characteristic grid cell, and some trees might be larger, but in either case, these objects are just momentum sinks within individual grid cells that require some drag coefficient that is appropriate to the local conditions.

2 Model Development

Consider a volume filled with a random collection of vegetative elements, like pine needles or leaves, as shown in Fig. 1. This volume can be regarded as a single grid cell in a CFD model for which the computational domain may span hundreds to thousands of meters. At a given instant in the numerical simulation, this grid cell would have, at the very least, an average flow speed, U, and gas density, ρ. The vegetation within the cell is typically modeled as a collection of subgrid-scale Lagrangian particles whose mass, size, and shape are characterized by a handful of parameters that can be determined with field measurements. These particles exert a force per unit volume given by:

$$F = \frac{N}{V_\mathrm{c}} \frac{\rho}{2} C_\mathrm{d} A_\mathrm{p} U^2 \tag{1}$$

where N is the number of elements, V_c is the volume of the grid cell, A_p is the projected area of a single element, and C_d is a drag coefficient. Similar configurations have already been been adapted in numerical investigations [7;8]. An alternative way to describe the vegetation is

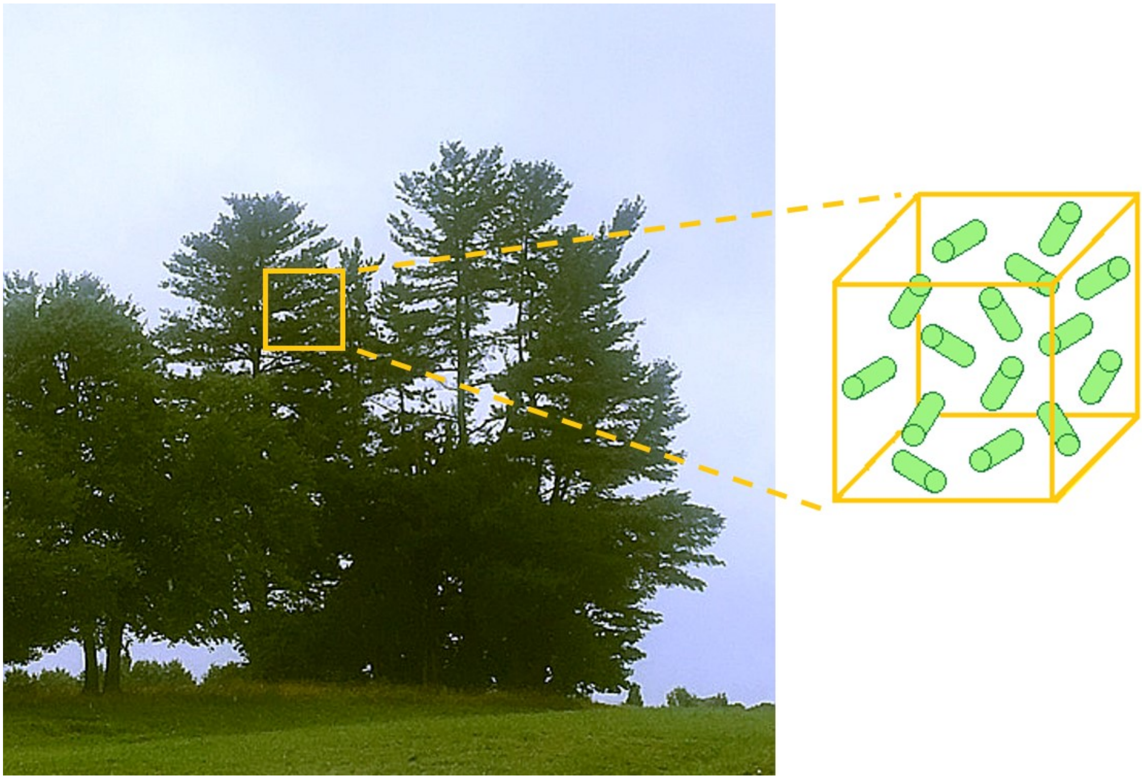

Fig. 1. Vegetation translation to multi-component model

by specifying the surface to volume ratio of each element, σ, the volume (packing) ratio of the collection of elements, β, and a shape factor, C_s, defined in this case as the ratio of the element's projected area to surface area. With this information, and the following relations:

$$C_\mathrm{s} = \frac{A_\mathrm{p}}{A_\mathrm{s}} \quad ; \quad \beta = \frac{N\,V_\mathrm{e}}{V_\mathrm{c}} \quad ; \quad \sigma = \frac{A_\mathrm{s}}{V_\mathrm{e}} \tag{2}$$

where V_e is the volume of an element and A_s its surface area, we can convert the drag force expression in Eq. (1) to an equivalent form [9]:

$$F = \frac{\rho}{2} C_\mathrm{d}\, C_\mathrm{s}\, \beta\, \sigma\, U^2 \tag{3}$$

Some of the terms are difficult to measure, such as the shape factor and surface to volume ratio, but collectively these terms may be combined into a single parameter:

$$\kappa = C_\mathrm{s}\, \beta\, \sigma \tag{4}$$

The parameter, κ, resembles an absorption coefficient* and can be determined by measuring the projected area of light, A, passing a given distance x through the vegetation. The decrease in the projected area of light is governed by the equation

$$\frac{\mathrm{d}A}{\mathrm{d}x} = -\kappa\, A \quad ; \quad A(x) = A(0)\,\mathrm{e}^{-\kappa x} \tag{5}$$

The relative fraction of light passing through a distance of L is

$$W = \frac{A(L)}{A(0)} = \mathrm{e}^{-\kappa L} \tag{6}$$

The parameter W is sometimes referred to as the "free-area coefficient" or "free-area fraction" in the literature.

In order to measure the drag coefficient, C_d, a section of length, L, of a small wind tunnel is to be filled with various amounts and types of vegetation and the pressure drop, ΔP, measured for an array of wind speeds, U. The value of κ shall be determined via black and white photography, and the drag coefficient extracted from the following form of the drag law derived above:

$$\frac{\Delta P}{L} = \frac{\rho}{2}\, C_\mathrm{d}\, \kappa\, U^2 \tag{7}$$

3 Description of Experiments

3.1 Sample Preparation

The vegetation chosen for this work was a Bakers Blue Spruce (*Picea pungens 'Bakeri'*), an Evergreen Distylium (Distylium 'PIIDIST-I'), a Gold Rider Leyland Cypress (*Cupressocyparis leylandii 'Gold Rider'*), a Kimberly Queen Fern (*Nephrolepis obliterata 'Kimberly Queen'*), a Blue Shag Eastern White Pine (*Pinus strobus 'Blue Shag'*), and a Robin Red Holly (*Ilex opaca*). Each sample was chosen based on its local availability. Leaf shapes were varied, including needle, elliptic, scale, and ovate.

The plant samples were cut into 0.5 m by 0.5 m by 0.5 m cubes using a guiding frame (left side of Fig. 2). The samples completely filled the cross section of the wind tunnel forcing the flow to move through the vegetation as opposed to around it. To easily distinguish the front, back, left, and right side of the cube-shaped vegetation, each side was designated Position A, B, C, or D (right side of Fig. 2). After its initial cut, image analysis, wind tunnel measurements, and water displacement testing were conducted in subsequent order. Image analysis and wind tunnel measurments were conducted for each position to obtain a collection of drag coefficients relative to different κ values. In some cases, samples were pruned and tested again. In the case of the Bakers Blue Spruce, Gold Rider Leyland Cypress, and Robin Red Holly, four prunings were made with the final one being the removal of all leaves.

3.2 Determining the Free-Area Coefficient via Photography

The free-area coefficient, W, was determined by placing each vegetation sample on a table located between a large white backdrop and a 0.5 m by 0.5 m cardboard frame, the same

*Another way to express κ using the relations in Eq. (2) is $NA_\mathrm{p}/V_\mathrm{c}$, or in other words, the total projected area per unit volume. This parameter describes the absorption of non-scattering light by solid particles using the same geometric assumption for thermal radiation absorption.

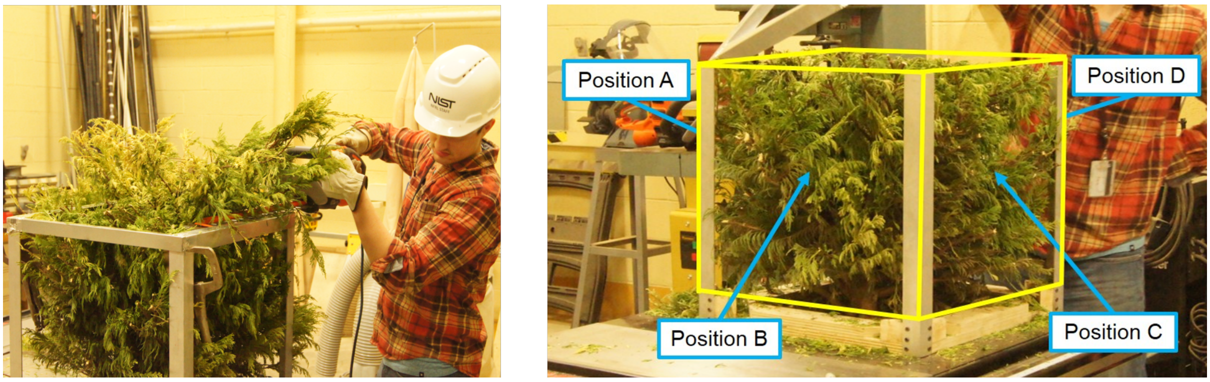

Fig. 2. Preparation of vegetation samples and designated orientation

dimensions as the tunnel cross section (Fig. 3). For each sample cut and position, the projected area was photographed. All images were captured using a Nikon D5600 camera† placed on a tripod located approximately 3.6 m away from the sample. The white backdrop was illuminated using a collection of incandescent and LED lights.

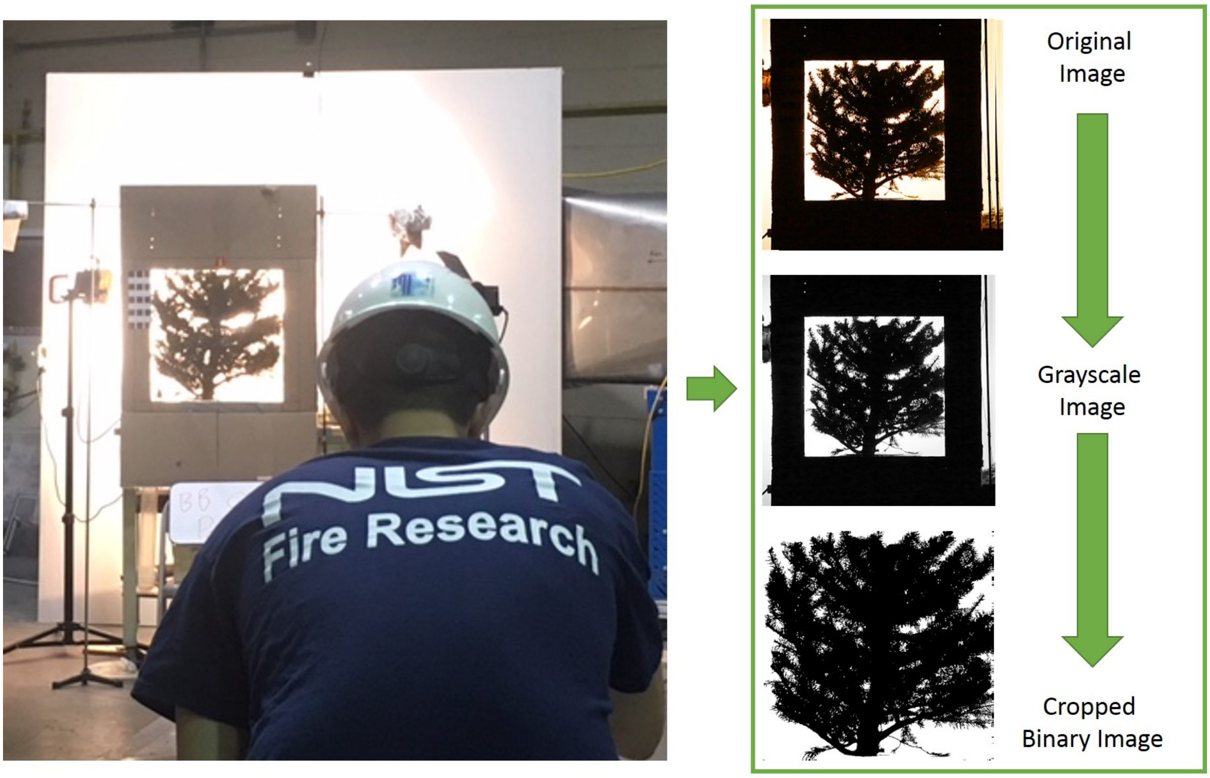

Fig. 3. Setup for photographing vegetation samples (left) and the post-processing procedure for analyzing images (right)

The images were processed using MATLAB's Image Processing Toolbox. Imported colored images were first converted into a grey scale and then a binary (black and white) image using a pre-set threshold level. The binary images were then cropped within the cardboard frame to eliminate non-vegetative substances and to evaluate the projected image of the vegetation exclusively. Once the projected image was obtained, a pixel count was conducted to determine

† Certain commercial products are identified in this report to specify adequately the equipment used. Such identification does not imply a recommendation by the National Institute of Standards and Technology, nor does it imply that this equipment is the best available for the purpose.

the free-area coefficient of the vegetation, W. Once obtained, the free-area coefficient was used to calculate κ from Eq. (6).

3.3 Description of the Wind Tunnel

Pressure loss measurements were obtained in a wind tunnel test section with a cross-sectional area of 0.5 m by 0.5 m and a length of 2 m. An image and schematic diagram of the wind tunnel setup is shown in Fig. 4. The volume flow through the tunnel was measured upstream of the vegetation using a Rosemont 485 annubar. The pressure drop across the vegetation was measured using an MKS Baratron Type 220D pressure transducer with a range of 0 to 133 Pa. The air flow was provided by a 0.91 m axial fan controlled by a variable frequency drive and monitored using the Annubar. Air density was calculated from pressure, temperature, and relative humidity readings of the testing facility. Each sample configuration was subjected to nine different fan speeds ranging from 0 to 88 % of the full-scale fan speed. The fan speed was not run at full scale due to the risk of exceeding the pressure transducer's pressure limitations. Data was sampled at 90 Hz for a 30 s period while maintaining a constant fan speed. Initially, pressure measurements were made at different lodations in front of and behind vegetation samples. However, no significant changes in the pressure drop across the vegetation was observed when moving the pressure taps.

Once a set of measurements was taken at all fan speeds, the wind tunnel was shut off for approximately 5 min, and then the measurements were repeated. All measurements were repeated three times for each vegetation configuration. The variance homogeneity of the replicate measurements was tested using Hartley's F_{max} test. If it was found that the data sets were homogenous, then the measurements were averaged.

3.4 Determining the Volume of Vegetation via Water Displacement

The volume of the vegetation was measured after a sample cut. The extracted vegetation was separated into branches and leaves and put into cloth mesh bags of known mass and volume, weighed, and submerged in a bucket. The displaced water flowed through a spout and into a beaker (Fig. 5). The measurement was repeated three times for each sample. The solid fraction, β, was calculated by dividing the average sample volume by the volume it occupied (0.5 m $\times$ 0.5 m $\times$ 0.5 m $= 0.125$ m^3).

4 Results

The key results of this work are the relationship between the absorption coefficient, κ, and the solid fraction, β, and the drag coefficient derived from the wind tunnel measurements. The accuracy of the results were verified by applying the same methods to a staggered tube bank configuration, detailed in Ref.[10]. A complete dataset of the results described in this manuscript is provided in Ref.[11].

4.1 Relationship between the Absorption Coefficient and Solid Fraction

Figure 6 presents the relationship between the averaged absorption coefficient, κ, and the solid fraction, β, for the sample configurations of the Bakers Blue Spruce, Evergreen Distylium, Gold Rider Leyland Cypress, and Robin Red Holly. The symbols indicate the measured values

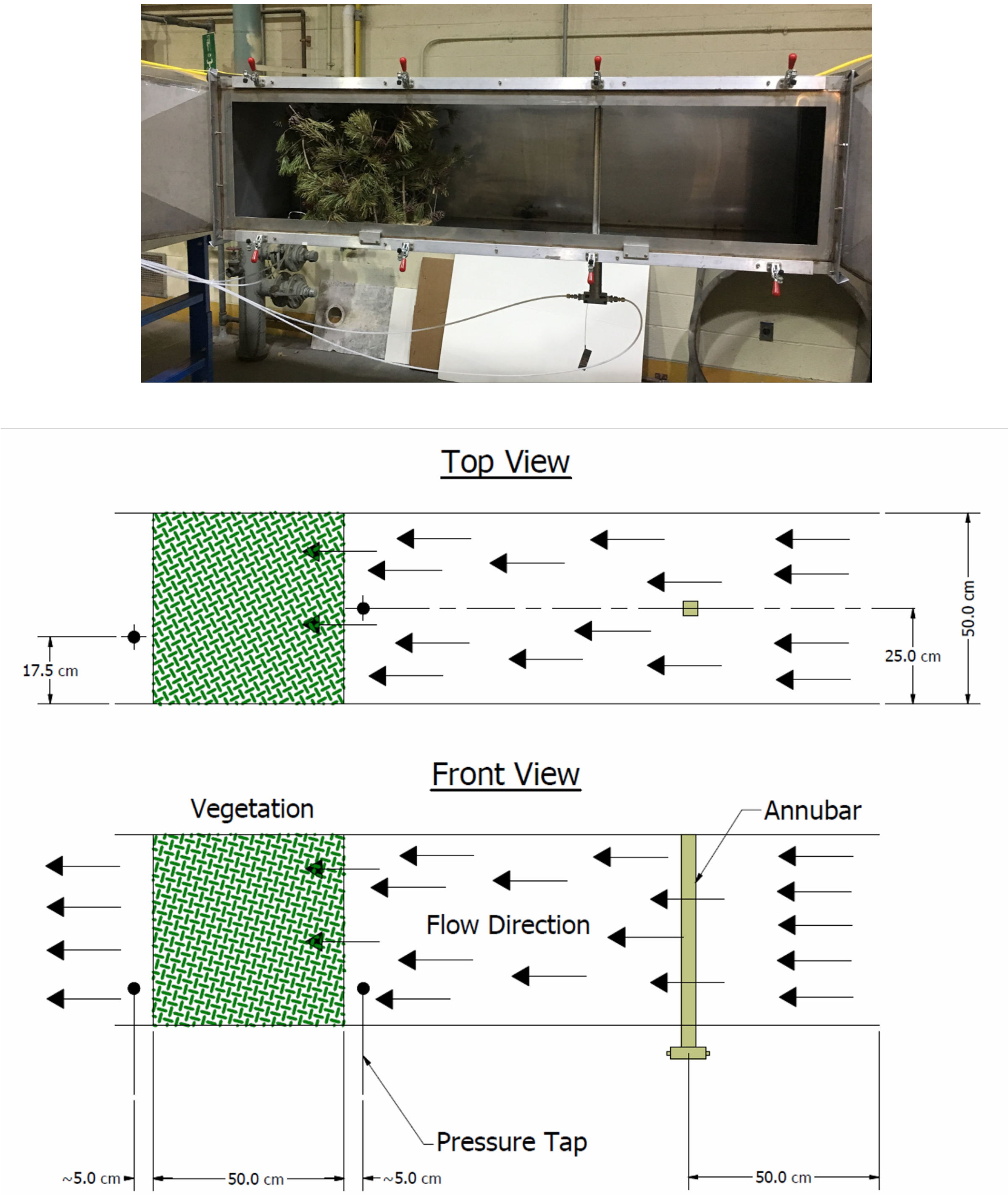

Fig. 4. Wind tunnel experimental setup with top and front schematic drawings

while the dotted lines represent a linear regression fit. Each line represents a particular type of vegetation that has been pruned, reducing both the volume fraction, β, the projected free-area coefficient, W, and the corresponding value of κ. There ought to be a linear relationship between κ and β if the shape factor, C_s, and surface to volume ratio, σ are constant, as shown in Eq. (4). However, this is not the case when the vegetative components are not uniform in size. Take, for example, the Robin Red Holly data shown in Fig. 6. As β decreases, κ should approach zero, as demonstrated by most samples. As the leaves of the Robin Red Holly were pruned, κ decreased significantly even though its volume fraction did not, owing to the fact the ratio of branch to leaf volume of the Robin Red Holly is substantially higher than the other

Fig. 5. Procedure of the water displacement test

plant species, as shown in Table 1. As a result, the free-surface area, W, decreases from the removal of leaves, thus reducing κ, while still maintaining a relatively consistent solid fraction due to the significant volume contribution of the branches.

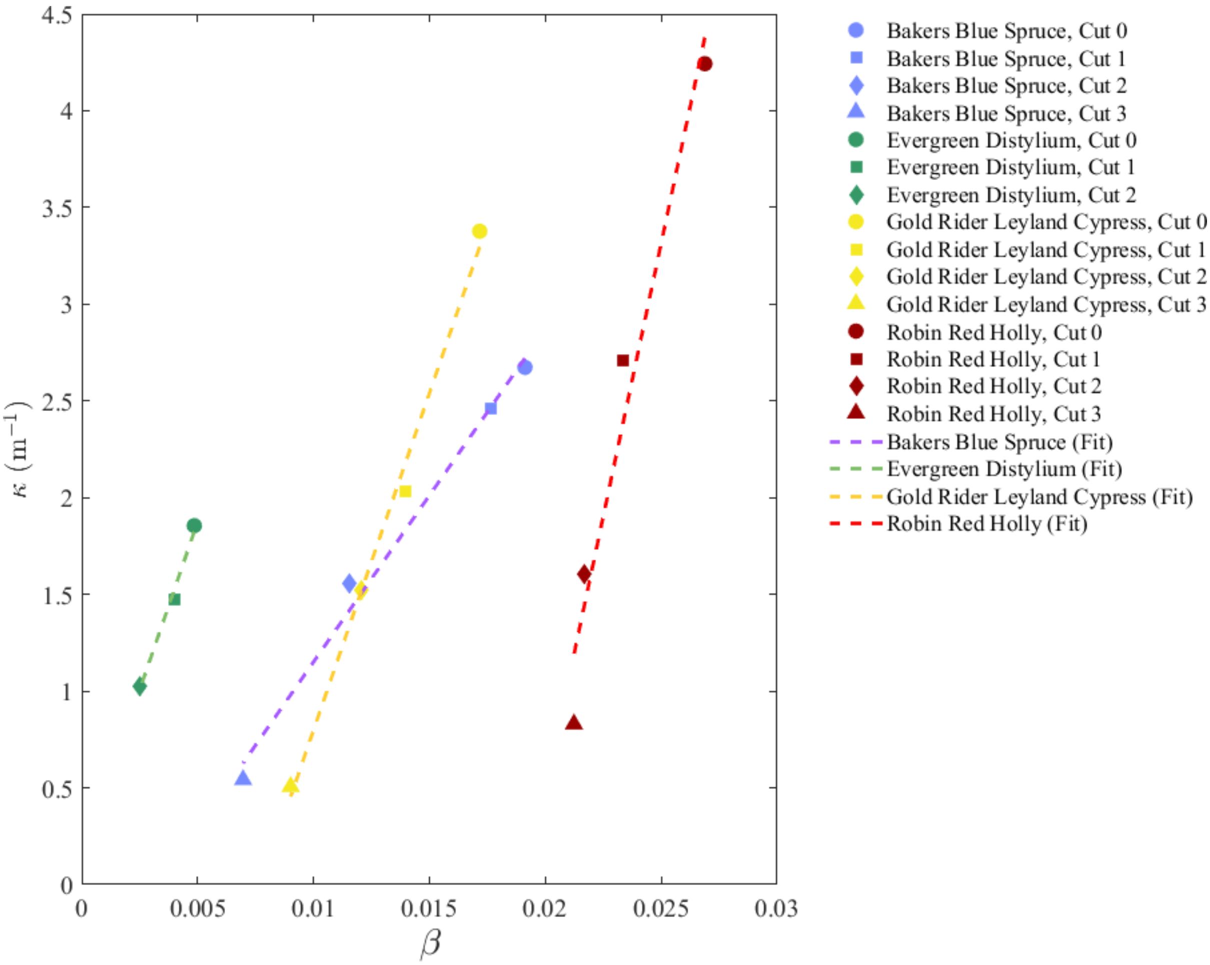

Fig. 6. Calculated absorption coefficient (κ) of vegetation sample configuration plotted against the corresponding solid fractions (β)

4.2 Vegetation Canopy Drag Coefficients

The left plot of Fig. 7 displays the relationship between the freestream velocity and the pressure drop for each sample configuration. The results demonstrate the expected quadratic relationship. Replotting the data as shown in the center plot of Fig. 7 yields the drag coefficient for each sample configuration as determined by calculating the slope of each line of data points. No linear regression fitting was observed to have a coefficient of determination less than 0.98, indicating a close representation of the fitted regression line to the measured data. A summary of all 68 calculated drag coefficients and their respective uncertainties are presented in Table 2. The procedure for determining the drag coefficient uncertainty as shown in this table can be found in a previously published technical report [10].

The distribution of the measured drag coefficients for all sample configurations is shown in Fig. 8. The collection of sample configurations is divided into two groups based on leaf shape (i.e., narrow and broad). The narrow leaves group included the Bakers Blue Spruce, Blue Shag Eastern White Pine, and Gold Rider Leyland Cypress while the broad leaves group was comprised of the remaining species. The average drag coefficient of all sample configurations was determined to be 2.8 with an expanded uncertainty of 0.4.

To determine if the average drag coefficient depends on the type of vegetation a random effects one-way Analysis of Variance (ANOVA) was implemented on the drag coefficients of the different vegetation samples. The analysis yielded a significant variation ($F(5,62) = 4.88$, $p = 7.97 \times 10^{-4}$) among the species[‡]. A Tukey's test [12] was subsequently applied to determine if the species-specific average drag coefficients were significantly different from each other. The results showed one significant difference between the species' average drag coefficients: the Robin Red Holly and Gold-Rider Leyland Cypress. Despite the significant difference, the average drag coefficients of these two plant species are still within the uncertainty bound of the overall drag coefficient and therefore are not large enough to have a practical implication.

Further analysis was conducted to compare the broad and narrow leaf shape groups. A one-way random effects model [13] for the measurements of the narrow leaves group assumes that the drag coefficients are normally distributed:

$$C_{\mathrm{d},ij} \sim N(m_1, {u_{ij}}^2 + {\sigma_1}^2),\ i = 1, ..., 3; j = 1, ..., n_i \tag{8}$$

where i denotes the plant species (1 for Bakers Blue Spruce, 2 for Blue Shag Eastern White Pine, and 3 for Gold Rider Leyland Cypress), and j denotes the specific configuration of the plant in the tunnel. The sample size for a given plant species is n_i. The value of u_{ij} is the standard uncertainty of the measured drag coefficient for a specific species and configuration. The parameters m_1 and σ_1 are the mean and standard deviation for the narrow leaves group, respectively. The drag measurements of the broad leaves group are modeled in a similar way:

$$C_{\mathrm{d},ij} \sim N(m_2, {u_{ij}}^2 + {\sigma_2}^2),\ i = 4, ..., 6; j = 1, ..., n_i \tag{9}$$

where $i = 4$ for Distylium, $i = 5$ for Fern, and $i = 6$ for Red Holly). The parameters m_2 and σ_2 are the mean and standard deviation for the broad leaves group, respectively.

Using a Bayesian statistical model [14] with non-informative priors for m_1, m_2, σ_1, and σ_2, we obtain via Markov Chain Monte Carlo implemented in OpenBUGS [15] the posterior means and

‡The F refers to the statistic obtained from the F-test conducted in the ANOVA, the 5 and 62 in brackets represent the degrees of freedom, and the 4.88 is the actual F statistic derived from the ANOVA. The p refers to the significance level determined from the F statistic and the 7.97×10^{-4} is the actual p-value which was determined to be less than the chosen confidence level of 0.05, indicating a significant difference between the mean drag coefficients of the samples.

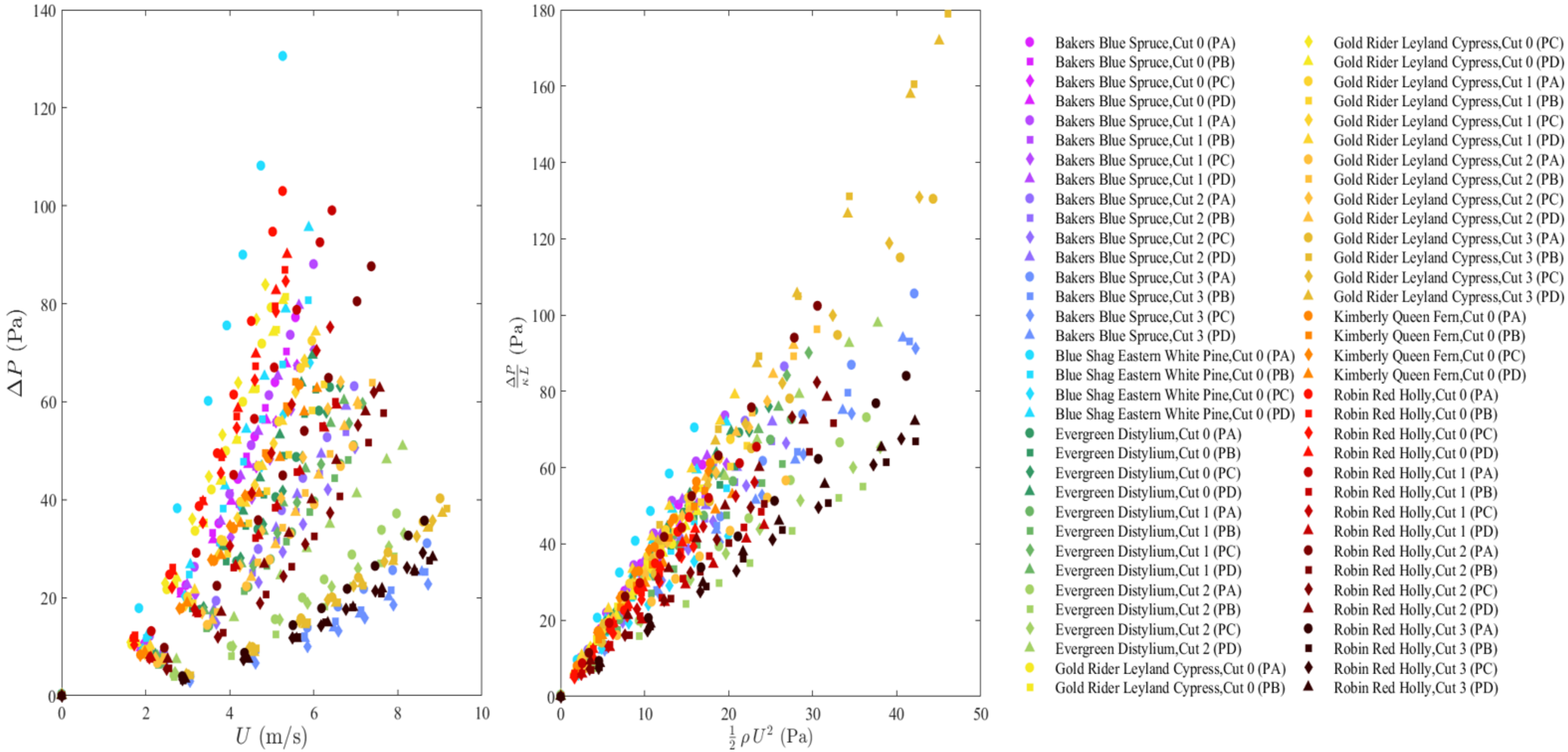

Fig. 7. Differential pressure measurments versus freestream velocity (left) and differential pressure over κ L versus dynamic pressure (center)

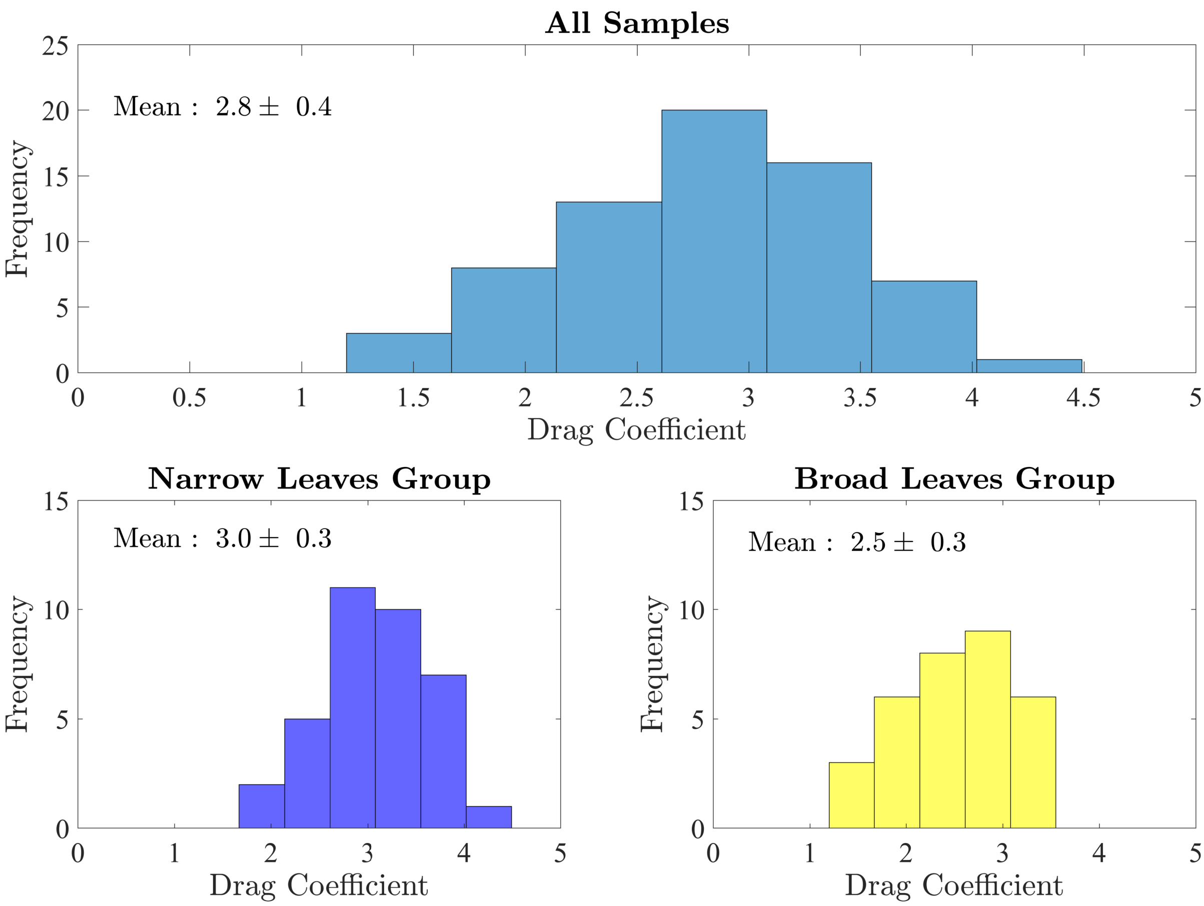

Fig. 8. Distribution of drag coefficients for all samples (top), samples with narrow leaves (bottom left), samples with broad leaves (bottom right).

standard uncertainties of the parameters. These are: m_1 is 3.0 with an expanded (95 %) uncertainty of 0.3, m_2 is 2.5 with an expanded (95 %) uncertainty of 0.3, and the 95 % uncertainty interval for the difference $m_1 - m_2$ is (0.052, 0.87). This may be interpreted as a rejection of a hypothesis test of $H_0\colon m_1 - m_2 = 0$ at a level of 5 %. Despite the differences in the average drag coefficients of both groups, they both lie within the uncertainty bound of the overall average drag coefficient, which suggests that mean drag coefficient obtained from all samples could be a reasonable approximation when applied as a consistent drag coefficient for vegetation canopies in CFD models.

5 Conclusion

This report documents a series of experiments implemented to determine the absorption coefficient, pressure loss, and the solid fraction of different types of vegetation sample configurations. The primary objective of this work was to calculate the drag coefficients of bulk vegetation that can be incorporated into CFD models. In addition to establishing drag coefficients of bulk vegetation, notable findings regarding vegetation structure and similarities between drag coefficients of plant species were also discovered from this work. It cannot be concluded, however, that the findings from this work applies to all bulk vegetation, but exclusively to the samples studied in these experiments.

To summarize, the findings of this work are as follows:

1. The calculated absorption coefficient for each sample demonstrated a strong relationship with its corresponding solid fraction.

2. The overall average drag coefficient of the bulk vegetation was found to be 2.8 with an expanded uncertainty of 0.4. The differences between the average drag coefficients of different plant species as well as the leaf type groups were shown to be significant, while still falling within the overall mean's uncertainty bound, suggesting that the overall average drag coefficient could be used as a constant value in CFD models of various plant types.

Acknowledgments

The authors would like to thank Maco Fernandez, Matthew Bundy, and Artur Chernovksy of the National Fire Research Laboratory at NIST and Blaza Tomen of the Statistical Design, Analysis, and Modeling Group at NIST, who assisted in conducting these experiments and in processing the data.

References

[1] McGrattan K., Hostikka S., McDermott R., Floyd J., Weinschenk C., Overholt K.. *Fire Dynamics Simulator, Technical Reference Guide.* National Institute of Standards and Technology, Gaithersburg, Maryland, USA, and VTT Technical Research Centre of Finland, Espoo, Finlandsixth ed. 2013. Vol. 1: Mathematical Model; Vol. 2: Verification Guide; Vol. 3: Validation Guide; Vol. 4: Software Quality Assurance.

[2] Cao J., Tamura Y., Yoshida A.. Wind tunnel study on aerodynamic characteristics of shrubby specimens of three tree species *Urban Forestry and Urban Greening.* 2012;11:465-476.

[3] Jalonen J., Järvelä J.. Estimation of drag forces caused by natural woody vegetation of different scales *J. Hydrodynamics.* 2014;26:608-623.

[4] Mayhead G.J.. Some Drag Coefficients for British Forest Trees Derived from Wind Tunnel Studies *Agricultural Meterology.* 1973;12:123-130.

[5] Gillies J. A.. Drag coefficient and plant form response to wind speed in three plant species: Burning Bush (Euonymus alatus), Colorado Blue Spruce (Picea pungens glauca.), and Fountain Grass (Pennisetum setaceum) *J. Geophysical Research.* 2002;107:ACL 10-1-ACL 10-15.

[6] Ishikawa H., Amano A. Suguru, Kenta Y.. Flow around a Living Tree *JSME International Journal, Series B: Fluids and Thermal Engineering.* 2006;49:1064-1069.

[7] Pimont F., Dupuy J.L., Linn R. R., Dupont S.. Validation of FIRETEC wind-flows over a canopy and a fuel-break *Int. J. Wildland Fire.* 2009;18:775-790.

[8] Dupont S., Brunet Y.. Edge flow and canopy structure: a large-eddy simulation study *Boundary Layer Meteorology.* 2008;126:51-71.

[9] Mueller E., Mell W., Simeoni A.. Large eddy simulation of forest canopy flow for wildland fire modeling *Canadian J. Forest Res..* 2014;44:1534-1544.

[10] Falkenstein-Smith R., McGrattan K., Toman B., Fernandez M.. Measurement of the Flow Resistance of Vegetation tech. rep.National Institute of Standards and Technology 2019.

[11] Falkenstein-Smith Ryan, McGrattan Kevin. Data set of Flow Resistance Measurements of Vegetation 2019. data retrieved from NIST Public Data Repository, `https://doi.org/10.18434/M31986`.

[12] Lane D., Salkin N.. Tukey's honestly significant difference (HSD) *N. Salkind der.), Encyclopedia of Research Design içinde, Thousand Oaks, CA: SAGE Publications.* 2010;1:1566–1571.

[13] Toman B., Possolo A.. Laboratory effects models for interlaboratory comparisons *Accreditation and Quality Assurance.* 2009;14:553-563.

[14] Gelman A., Carlin J., Stern H., Rubin D.. *Bayesian Data Analysis, 2nd Edition.* Chapman and Hall/CRC 2013.

[15] Lunn David, Spiegelhalter David, Thomas Andrew, Best Nicky. The BUGS project: Evolution, critique and future directions *Statistics in medicine.* 2009;28:3049–3067.

Table 1. Branch and leaf volume ratio of vegetation samples with mulitple cut iterations

Sample	β (%)	**Branch/Leaf Vol.**	**Sample**	β (%)	**Branch/Leaf Vol.**
Blue Spruce	1.9	1.1	Cypress	1.7	1.5
	1.8	1.3		1.4	2.2
	1.2	1.5		1.2	3.0
	0.7	N/A		0.9	N/A
Distylium	0.5	1.0	Red Holly	2.7	11
	0.4	1.4		2.3	16
	0.3	3.3		2.2	47
				2.1	N/A

Table 2. Drag coefficient summary of vegetation samples

Sample	β (%)	**Position**	C_d	**Uncertainty**	**Sample**	β (%)	**Position**	C_d	**Uncertainty**
Blue Spruce	1.9	A	3.6	0.5	Cypress	1.7	A	3.0	0.5
		B	3.1	0.5			B	3.2	0.5
		C	3.1	0.4			C	3.4	0.5
		D	3.0	0.4			D	3.0	0.4
	1.8	A	3.8	0.5		1.4	A	3.3	0.4
		B	3.0	0.4			B	2.9	0.4
		C	3.1	0.4			C	3.3	0.4
		D	3.6	0.4			D	3.8	0.4
	1.2	A	3.2	0.4		1.2	A	2.1	0.5
		B	2.6	0.3			B	3.2	0.3
		C	2.5	0.3			C	3.1	0.4
		D	2.8	0.3			D	3.3	0.4
	0.7	A	2.5	0.4		0.9	A	2.9	0.4
		B	2.3	0.4			B	3.9	0.4
		C	2.2	0.4			C	3.0	0.5
		D	2.2	0.4			D	3.8	0.5
White Pine	2.8	A	4.4	0.7	Fern	0.4	A	3.4	0.5
		B	2.8	0.4			B	3.1	0.4
		C	2.1	0.4			C	3.3	0.5
		D	3.6	0.5			D	2.6	0.4
Distylium	0.5	A	3.2	0.4	Red Holly	2.7	A	3.1	0.5
		B	2.9	0.4			B	2.6	0.4
		C	3.1	0.4			C	2.5	0.4
		D	3.4	0.4			D	2.7	0.4
	0.4	A	2.7	0.3		2.3	A	2.8	0.4
		B	2.3	0.3			B	2.0	0.3
		C	3.1	0.4			C	2.5	0.3
		D	2.9	0.4			D	1.8	0.3
	0.3	A	2.0	0.3		2.2	A	3.4	0.3
		B	1.5	0.2			B	2.2	0.2
		C	1.7	0.3			C	2.7	0.3
		D	2.6	0.3			D	2.5	0.3
						2.1	A	2.1	0.3
							B	1.6	0.3
							C	1.6	0.3
							D	1.7	0.3